

Binary Lenses in OGLE III EWS Database. Season 2005

by

J. S k o w r o n, M. J a r o s z y ń s k i, A. U d a l s k i,
M. K u b i a k, M.K. S z y m a ń s k i, G. P i e t r z y ń s k i,
I. S o s z y ń s k i, O. S z e w c z y k, Ł. W y r z y k o w s k i
and K. U l a c z y k

Warsaw University Observatory, Al. Ujazdowskie 4, 00-478 Warszawa, Poland

e-mail:

(jskowron,mj,udalski,mk,msz,pietrzyn,soszynsk,szewczyk,wyrzykow,ulaczyk)
@astrouw.edu.pl

ABSTRACT

We present nine new binary lens candidates from OGLE-III Early Warning System database for the season of 2005. We have also found four events interpreted as single mass lensing of double sources. The candidates have been selected by visual light curves inspection. Examining the models of binary lenses in our previous studies (10 caustic crossing events of OGLE-II seasons 1997–1999 and 34 binary lens events of OGLE-III seasons 2002–2004, including one planetary event), in this work and in three publications concerning planetary events of season 2005, we find four cases of extreme mass ratio binaries ($q \leq 0.01$), and almost all other models with mass ratios in the range $0.1 < q < 1.0$, which may indicate the division between planetary systems and binary stars.

Key words: *Gravitational lensing – Galaxy: center – binaries: general*

1. Introduction

In this paper we present the results of the search for binary lens events among microlensing phenomena discovered by the Early Warning System (EWS – Udalski *et al.* 1994, Udalski 2003) of the third phase of the Optical Gravitational Lensing Experiment (OGLE-III) in the season of 2005. This is a continuation of the study of binary lenses in OGLE-II (Jaroszyński 2002, hereafter Paper I) and OGLE-III databases (Jaroszyński *et al.* 2004, hereafter Paper II and Jaroszyński *et al.* 2006, hereafter Paper III). The results of the similar search for binary lens events in MACHO data were presented by Alcock *et al.* (2000).

The motivation of the study remains the same – we are going to obtain a uniform sample of binary lens events, selected and modeled with the same methods for all seasons. The sample may be used to study the population of binary systems

in the Galaxy. The method of observation of the binaries (gravitational lensing) allows to study their mass ratios distribution, since they are directly given by the models. The binary separations are more difficult, because only their projection into the sky expressed in Einstein radius units enters the models. In small number of cases the estimation of the masses and distances to the lenses may be possible.

Cases of extremely low binary mass ratios ($q \leq 0.01$) are usually considered as planetary lensing. Such events have been discovered in OGLE-III database for season 2003 (Bond *et al.* 2004), 2005 (Udalski *et al.* 2005, Gould *et al.* 2006, Beaulieu *et al.* 2006), and 2007 (to be published). The adequate modeling of a planetary event requires frequent round the clock observations of the source, which is achieved by cooperation of observers at different longitudes on Earth. In cases of less extreme lenses, the observations of single telescope may be sufficient to obtain well constrained models of the systems. The present analysis is based on the OGLE-III data alone.

Our approach follows that of Papers I, II, and III, where the references to earlier work on the subject are given. Some basic ideas for binary lens analysis can be found in the review article by Paczyński (1996). Paper I presents the analysis of 18 binary lens events found in OGLE-II data with 10 safe caustic crossing cases. There are 15 binary lens events reported in Paper II, and 19 in Paper III.

In Section 2 we describe the selection of binary lens candidates. In Section 3 we describe the procedure of fitting models to the data. The results are described in Section 4, and the discussion follows in Section 5. The extensive graphical material is shown in Appendix.

2. Choice of Candidates

The OGLE-III data are routinely reduced with difference photometry (DIA, Alard and Lupton 1998, Alard 2000) which gives high quality light curves of variable objects. The EWS system of OGLE-III (Udalski 2003) automatically picks up candidate objects with microlensing-like variability.

There are 597 microlensing event candidates selected by EWS in the 2005 season. We visually inspect all candidate light curves looking for features characteristic for binary lenses (multiple peaks, U-shapes, asymmetry). Light curves showing excessive noise are omitted. We select 12 candidate binary events in 2005 data for further study. For these candidate events we apply our standard procedure of finding binary lens models (*cf.* Papers I–III and Section 3).

3. Fitting Binary Lens Models

The models of the two point mass lens were investigated by many authors (Schneider and Weiss 1986, Mao and DiStefano 1995, DiStefano and Mao 1996, Dominik

1998, to mention only a few). The effective methods applicable for extended sources were described by Mao and Loeb (2001). We follow their approach and use image finding algorithms based on the Newton method. Our implementation of adaptive contouring approach to image finding (Dominik 2007) proved more time consuming, and has not been used.

We fit binary lens models using the χ^2 minimization method for the light curves. It is convenient to model the flux at the time t_i as:

$$F_i = F(t_i) = A(t_i) \times F_s + F_b \equiv (A(t_i) - 1) \times F_s + F_0 \quad (1)$$

where F_s is the flux of the source being lensed, F_b the blended flux (from the source close neighbors and possibly the lens), and the combination $F_b + F_s = F_0$ is the total flux at baseline, measured long before or long after the event. The last parameter can be reasonably well estimated with observations performed in seasons preceding and following 2005, as a weighted mean:

$$F_0 = \frac{\sum_{i'=1}^{N'} \frac{F_i}{\sigma_i}}{\sum_{i'=1}^{N'} \frac{1}{\sigma_i}} \quad (2)$$

where F_i are the observed fluxes and σ_i their estimated photometric errors. The summation over i' does not include observations of 2005, and N' is the number of relevant observations.

In fitting the models we use rescaled errors (compare Papers I–III). More detailed analysis (*e.g.*, Wyrzykowski 2005) shows that the OGLE photometric errors are overestimated for very faint sources and underestimated for bright ones. Error scaling used here, based on the scatter of the source flux in seasons when it is supposedly invariable, is the simplest approach. It gives the estimate of the combined effect of the observational errors and possibly undetectable, low amplitude internal source variability. We require that constant flux source model fits well the other seasons data after introducing error scaling factor s :

$$\chi_{\text{other}}^2 = \sum_{i'=1}^{N'} \frac{(F_i - F_0)^2}{(s\sigma_i)^2} = N' - 1. \quad (3)$$

The lens magnification (amplification) of the source $A(t_i) = A(t_i; p_j)$ depends on the set of model parameters p_j . Using this notation one has for the χ^2 :

$$\chi^2 = \sum_{i=1}^N \frac{((A_i - 1)F_s + F_0 - F_i)^2}{\sigma_i^2}. \quad (4)$$

The dependence of χ^2 on the binary lens parameters p_j is complicated, while the dependence on the source flux is quadratic. The equation $\partial\chi^2/\partial F_s = 0$ can be

solved algebraically, giving $F_s = F_s(p_j; \{F_i\})$, thus effectively reducing the dimension of parameter space. Any method of minimizing χ^2 may (in some cases) give unphysical solutions with $F_s > F_0$, which would imply a negative blended flux. To reduce the occurrence of such faulty solutions we add an extra term to χ^2 which vanishes automatically for physically correct models with $F_s \leq F_0$, but is a fast growing function of the source flux F_s whenever it exceeds the base flux F_0 .

Our analysis of the models, their fit quality etc. is based on the χ_1^2 calculated with the rescaled errors:

$$\chi_1^2 \equiv \frac{\chi^2}{s^2} \quad (5)$$

which is displayed in the tables and plots. For events with multiple models (representing different local minima of χ^2), we assess the relevance of each model with the relative weight $w \sim \exp(-\chi_1^2/2)$.

The number of events with at least one well sampled caustic crossing is relatively high among 2005 binary lens candidates, so the extended source models can be fitted. The extended source models may seem more difficult, but looking for the χ^2 minima may be easier in this case. The light curves for point sources have (formally) infinite jumps on caustic crossings. This implies that a small change in model parameters may drastically change the synthetic light curve shape and the quality of the fit. For extended sources the model light curves are continuous which substantially diminishes the problem. This property may be exploited in two ways. First, postulating a very large source radius one obtains an almost smooth χ^2 dependence on other parameters, with much lower number of local minima, which may help in the initial stages of optimization. On the other hand the optimization of a model with slightly perturbed source size, may lead to a better fitted new solution. The latter approach is easy to implement and control and we use it routinely.

The binary system consists of two masses m_1 and m_2 , where by convention $m_1 \leq m_2$. The Einstein radius of the binary lens is defined as:

$$r_E = \sqrt{\frac{4G(m_1 + m_2)}{c^2} \frac{d_{OL}d_{LS}}{d_{OS}}} \quad (6)$$

where G is the constant of gravity, c is the speed of light, d_{OL} is the observer–lens distance, d_{LS} is the lens–source distance, and $d_{OS} \equiv d_{OL} + d_{LS}$ is the distance between the observer and the source. The Einstein radius serves as a length unit and the Einstein time: $t_E = r_E/v_\perp$, where v_\perp is the lens velocity relative to the line joining the observer with the source, serves as a time unit. The passage of the source in the lens background is defined by seven parameters: $q \equiv m_1/m_2$ ($0 < q \leq 1$) – the binary mass ratio, d – binary separation expressed in r_E units, β – the angle between the source trajectory as projected onto the sky and the projection of the binary axis, b – the impact parameter relative to the binary center of mass, t_0 – the time of closest approach of the source to the binary center of mass, t_E – the

Einstein time, and r_s the source radius. Thus we are left with the seven or six dimensional parameter space, depending on the presence/absence of observations covering the caustic crossings.

We begin with a scan of the parameter space using a logarithmic grid of points in (q, d) plane ($10^{-3} \leq q \leq 1$, $0.1 \leq d \leq 10$) and allowing for continuous variation of the other parameters. The choice of starting points combines systematic and Monte Carlo searching of regions in parameter space allowing for caustic crossing or cusp approaching events. The χ^2 minimization is based on downhill method and uses standard numerical algorithms. When a local minimum is found we make a small Monte Carlo jump in the parameter space and repeat the downhill search. In some cases it allows for finding a different local minimum. If it does not work several times, we stop and try next starting point.

Some models may be improved by taking into account parallax effects and/or the changes in the orientation and separation of the binary lens caused by its rotation. The parallax parameter:

$$\pi_E = \frac{1 \text{ a.u.}}{\tilde{r}_E} \quad \tilde{r}_E = r_E \frac{d_{OS}}{d_{LS}} \quad (7)$$

where \tilde{r}_E is the radius of the Einstein ring projected into the observer's plane, measures the influence of the Earth motion on the source path relative to the lens position. Another parameter defines the orientation of the source path relative to the Ecliptic. In the linear approximation the lens rotation may be described as:

$$d = d_0 + \dot{d}(t - t_0) \quad \beta = \beta_0 + \dot{\beta}(t - t_0) \quad (8)$$

where the subscript “0” denotes values of parameters measured when the source approaches the binary center of mass. (The detailed definitions of all binary lens parameters when parallax and rotation are taken into account are given by Jaroszyński *et al.* 2005).

Only the events with characteristics of caustic crossing (apparent discontinuities in observed light curves, U-shapes) can be treated as safe binary lens cases. The double peak events may result from cusp approaches, but may also be produced by double sources (*e.g.*, Gaudi and Han 2004). In such cases we also check the double source fit of the event postulating:

$$F(t) = A(u_1(t)) \times F_{s1} + A(u_2(t)) \times F_{s2} + F_b \quad (9)$$

where F_{s1} , F_{s2} are the fluxes of the source components, F_b is the blended flux, and $A(u)$ is the single lens amplification. In most cases the formula for a point source amplification (Paczynski 1986) is sufficient, but the influence of the source finite size may show up, when the amplification is extreme. We routinely take this effect into account. The dimensionless source-lens separations are given as:

$$u_1(t) = \sqrt{b_1^2 + \frac{(t - t_{01})^2}{t_E^2}} \quad u_2(t) = \sqrt{b_2^2 + \frac{(t - t_{02})^2}{t_E^2}} \quad (10)$$

where t_{01} , t_{02} are the closest approach times of the source components, b_1 , b_2 are the respective impact parameters, and t_E is the (common) Einstein time.

4. Results

Our fitting procedures applied to 12 candidate events selected give the results summarized in Table 1. (We do not include the published models of planetary events. While for the event OGLE 2005-BLG-071 the modeling based on OGLE data alone is possible and gives results consistent with the final model based on combined observations from many telescopes, such an approach is not possible for OGLE 2005-BLG-169 or OGLE 2005-BLG-390.)

Table 1
Binary lenses parameters, excluding known planetary cases

Event		χ^2_1/DOF	s	q	d	β	b	t_0	t_E	f	r_s	π_E
017	d	902.8/393	1.71	0.061	1.229	155.22	-0.14	3456.5	57.9	0.55		
017	d	1032.6/392	1.71	0.002	1.018	141.69	0.07	3456.6	73.2	0.28		
018	b	6190.2/491	1.73	0.516	0.726	253.43	0.12	3513.0	55.5	1.00	0.0237	0.08
062	b	720.1/370	1.57	0.691	2.065	128.29	-0.12	3479.6	34.7	1.00		
128	b	467.7/309	1.03	0.852	1.606	200.29	-0.03	3511.2	50.3	0.47		
153	b	1395.4/467	2.88	0.806	0.830	209.02	0.53	3544.5	32.1	0.96	0.0160	0.59
189	b	1023.7/771	1.04	0.790	0.842	166.02	0.75	3526.4	98.7	0.96	0.0011	
226	b	607.3/353	1.13	0.284	0.296	96.86	0.02	3573.7	37.5	0.81	0.0088	
327	b	836.8/441	1.09	0.810	0.566	260.05	0.14	3566.2	112.6	1.00	0.0008	0.19
327	b	885.6/441	1.09	0.099	3.277	60.82	2.40	4208.9	477.3	0.97	0.0002	0.02
331	?	22752.0/462	1.66	0.199	0.872	111.59	0.08	3562.6	17.8	0.69		
463	b	666.4/413	1.25	0.120	1.538	83.90	0.82	3600.5	72.2	0.38		
468	b	378.5/261	1.21	0.529	0.440	55.23	0.00	3592.3	52.9	0.05	0.0005	
477	d	572.7/403	1.32	0.009	1.374	186.97	-0.05	3630.4	84.9	0.27		

Note: The table contains all 2005 season events, which have been modeled as binary lenses. The columns show: the event 2005 EWS number, the event classification (“b” for binary lens, “d” for double source, “?” for unknown), the rescaled χ^2_1 , number of DOF, the scaling factor s ($\chi^2_1 = \chi^2_{\text{raw}}/s^2$), the mass ratio q , the binary separation d , the source trajectory direction β , the impact parameter b , the time of the closest center of mass approach t_0 , the Einstein time t_E and the blending parameter $f \equiv F_s/F_0$. For events with resolved caustic crossings the size of the source r_s is given; otherwise it is omitted. Models taking into account the parallax effects have assigned value of the parameter π_E .

In the second column of Table 1 we assess the character of the events. In 9 cases (of 12 investigated) the events are safe binary lens phenomena in our opinion (designated as “b” in Table 1). There are 2 cases classified as double source events (“d” in Table 1) and 1 event with a low quality fit (“?” in Table 1). The source paths and model light curves are shown in the first part of Appendix.

In modeling of the event OGLE 2005-BLG-018 we have been forced to include parallax and rotation effects. The light curve of this event shows a smooth peak near Julian date 2 453 460 and two asymmetric tall peaks ≈ 50 days and ≈ 70 days

later. The sharp bend of the light curve before the second tall peak implies that the source is entering the caustic here, so the tall peaks may be interpreted as two separate enterings into the caustic region by a large source. The trajectory should also approach a cusp to obtain the smaller observed peak. Our model fits all the observed features qualitatively well.

In a few other cases the inclusion of the parallax effect has given models of substantially better formal quality (χ^2_1 smaller by at least 50). For such models the value of the parallax parameter is included in Table 1. In the remaining cases the parallax has no significant effect.

The results of double source modeling are summarized in Table 2. The double source modeling is applied to all binary lens candidates and some other non-standard events. While formally the fits are usually better for binary lenses, in two cases we prefer double source models as more natural, giving less complicated light curves. The comparison of two kinds of fits is given in the second part of Appendix, and the well separated double source events – in the third.

Table 2
Parameters of double source modeling

Event		χ^2_1/DOF	b_1	b_2	t_{01}	t_{02}	t_E	f_1	f_2
017	d	973./393	0.0039	0.0956	3455.75	3456.38	78.0	0.007	0.270
018	b	359081./490	0.0000	0.0000	3512.44	3528.89	130.7	0.074	0.092
062	b	2741./363	0.1999	0.0019	3460.68	3476.40	64.1	0.162	0.030
066	d	419./312	0.0095	0.0204	3439.10	3448.92	165.0	0.015	0.024
128	b	5554./310	0.1577	0.1091	3495.45	3538.23	44.2	0.443	0.314
153	b	475463./470	0.0016	0.0000	3557.46	3560.65	313.7	0.011	0.001
189	b	2945./772	0.0264	0.0000	3502.08	3512.75	252.8	0.068	0.002
192	d	687./383	1.7234	0.0158	3516.13	3529.50	27.1	0.994	0.006
226	b	26557./354	0.0755	0.0000	3573.31	3573.71	34.7	0.824	0.176
327	b	133339./348	0.0000	0.0000	3575.25	3579.62	74.4	0.184	0.317
331	?	10785./433	0.0000	0.1561	3554.27	3560.16	27.7	0.141	0.859
463	b	84000./415	0.0000	0.0000	3585.86	3609.45	312.1	0.003	0.021
468	b	7596./231	0.0230	0.0000	3589.65	3594.56	17.0	0.126	0.004
477	d	521./404	0.0599	0.0128	3629.02	3663.12	67.8	0.336	0.033

Note: The table contains the event number in 2005 EWS database, the classification of the event, the rescaled χ^2 value and the DOF number, the impact parameters b_1 and b_2 for the two source components, times of the closest approaches t_{01} and t_{02} , the Einstein time t_E , and the blending parameters $f_1 = F_{s1}/(F_{s1} + F_{s2} + F_b)$ and $f_2 = F_{s2}/(F_{s1} + F_{s2} + F_b)$.

Our sample of binary lenses consists now of $10 + 15 + 19 + 9 + 3 = 56$ events of Papers I–III, and the present work, some of them with multiple models, plus three published planetary events of the season 2005, which we also include. Using the sample we study the distributions of various binary lens parameters. In Fig. 1 we show the histograms for the mass ratio and the binary separation. The mass ratio is practically limited to the range $0.1 \leq q \leq 1$ with very small probability of finding

a model in the range $0.01 \rightarrow 0.1$. The four published planetary lens events are also included.

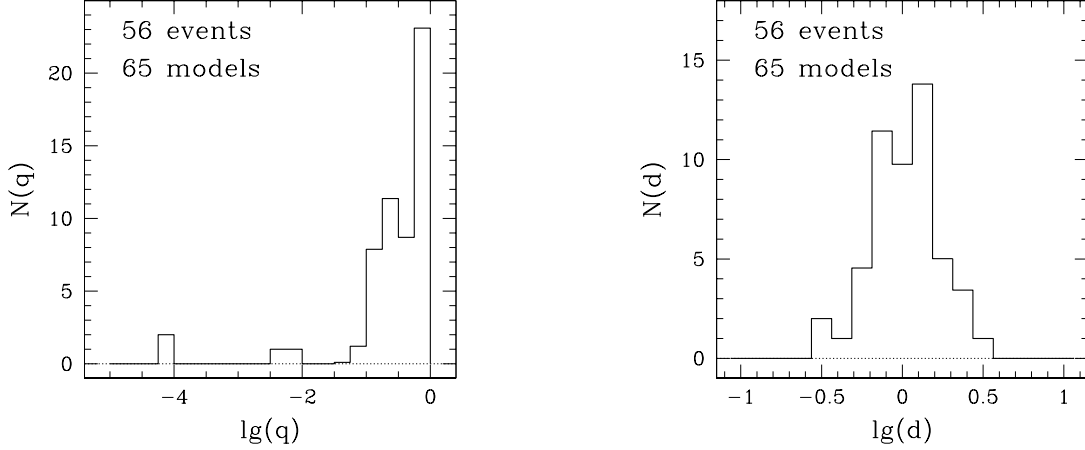


Fig. 1. The histogram of mass ratios (*left*) and separations (*right*) for binary lens events of OGLE-II (Paper I) and OGLE-III (Paper II, III, and this work). The histogram includes 56 events, some of them with multiple models. The alternative models of any event have been assigned fractional weights.

5. Discussion

The caustic crossing events dominate our sample of binary lenses. According to Night, DiStefano and Schwamb (2007) the number of caustic crossing and other events caused by binary lenses should be comparable. This claim is based on simulation investigating binary lenses of various mass ratios and separations, and source paths with different impact parameters and directions relative to the binary. The simulated light curves with some noise added are then checked algorithmically for differences relative to a point lens light curve, asymmetry, and multiple peaks. Cases which at the assumed level of “observational” noise can be classified as binary lenses, are then subdivided into smooth and caustic crossing categories with similar counts. We do not object to this conclusion, however our aim is to obtain well constrained models of the lenses, not the list of events which cannot be modeled as point lenses. The similarity between lensing of a double source and some cases of binary lensing can be seen in Appendix, and Papers II and III. Another example – OGLE 2005-BLG-055 (Jaroszyński and Paczyński 2002) – is also not a point lens case, but its binary lens model is completely unconstrained. This shows, that events with well marked deviations from point lens light curves (*e.g.*, chosen by visual inspection) have better chance of getting well constrained models. Since caustic crossing events usually imply large deviations from single peak, smooth light curves characteristic for point lens events, they also outnumber other kinds of events in our sample.

Our models of the events OGLE 2005-BLG-018 and OGLE 2005-BLG-153 have the highest χ^2_1/DOF ratio. Simultaneously the model light curves reproduce all changes of the observed flux quite well. Both sources reach very high apparent luminosities ($I \approx 12$ mag) due to the lens amplification and in the most interesting time interval are observed many times during each night. Our method of errors scaling based on the flux scatter at the baseline is not sufficient in these cases. The application of Wyrzykowski (2005) error scaling improves the formal quality of the models substantially, but not completely. The problem may be partially due to the limb darkening of the source, which we do not include in our models.

Our classification of the investigated events into the binary lens double source/unknown categories needs further explanation. The formally best binary lens model of the event OGLE 2005-BLG-017 does not reflect the bending of the observed light curve during the nights with Julian dates 3456–3459. Other models which fit this part of the light curve much better, have unacceptable quality at earlier epochs (compare Appendix and Table 1). The double source fit is formally better, but the bend of the light curve is also not well modeled in this case. The double source model of the event OGLE 2005-BLG-477 is quantitatively better. The best binary lens model gives a comparable fit to the data but it predicts a caustic crossing during unobserved period of winter 2005/2006, which we treat as an unwanted, not verifiable property of the model.

Our sample of OGLE binary lens events contains now 56 cases. The bimodality of the mass ratio distribution and the lack of intermediate q values remains a valid interpretation of the data. We are not trying a statistical interpretation of mass ratio distribution in this paper skipping it into a further publications.

Acknowledgements. We thank Shude Mao for the permission of using his binary lens modeling software. This work was supported in part by MNiSW grants N203 008 32/0709 and N203 030 32/4275. JS and LW acknowledge support of the European Community’s Sixth Framework Marie Curie Research Training Network Programme, Contract No. MRTN-CT-2004-505183 “ANGLES”.

REFERENCES

- Alard, C. 2000, *Astron. Astrophys. Suppl. Ser.*, **144**, 363.
 Alard, C., and Lupton, R.H. 1998, *Astrophys. J.*, **503**, 325.
 Albrow, M.D., *et al.* 1999, *Astrophys. J.*, **522**, 1022.
 Alcock, C., *et al.* 2000, *Astrophys. J.*, **541**, 270.
 An, J.H., *et al.* 2002, *Astrophys. J.*, **572**, 521.
 Beaulieu, J.-P., *et al.* 2006, *Nature*, **439**, 437.
 Bond, I.A., *et al.* 2004, *Astrophys. J. Letters*, **606**, L155.
 DiStefano, R., and Mao, S. 1996, *Astrophys. J.*, **457**, 93.
 Dominik, M. 1998, *Astron. Astrophys.*, **333**, L79.
 Dominik, M. 2007, *MNRAS*, **377**, 1679.
 Gaudi, B.S. and Han, Ch. 2004, *Astrophys. J.*, **611**, 528.

- Gould, A., *et al.* 2006, *Astrophys. J. Letters*, **644**, L37.
- Jaroszyński, M. 2002, *Acta Astron.*, **52**, 39 (Paper I).
- Jaroszyński, M., and Paczyński, B. 2002, *Acta Astron.*, **52**, 361.
- Jaroszyński, M., Udalski, A., Kubiak, M., Szymański, M., Pietrzyński, G., Soszyński, I., Żebruń, K., Szewczyk, O., and Wyrzykowski, Ł. 2004, *Acta Astron.*, **54**, 103 (Paper II).
- Jaroszyński, M., Udalski, A., Kubiak, M., Szymański, M., Pietrzyński, G., Soszyński, I., Żebruń, K., Szewczyk, O., and Wyrzykowski, Ł. 2005, *Acta Astron.*, **55**, 159.
- Jaroszyński, M., Skowron, J., Udalski, A., Kubiak, M., Szymański, M., Pietrzyński, G., Soszyński, I., Żebruń, K., Szewczyk, O., and Wyrzykowski, Ł. 2006, *Acta Astron.*, **56**, 307 (Paper III).
- Mao, S., and DiStefano, R. 1995, *Astrophys. J.*, **440**, 22.
- Mao, S., and Loeb, A. 2001, *Astrophys. J. Letters*, **547**, L97.
- Night, Ch., DiStefano, R., and Schwamb, M. 2007, *Astrophys. J.*, submitted (astro-ph/0705.0169).
- Paczynski, B. 1996, *Ann. Rev. Astron. Astrophys.*, **34**, 419.
- Schneider, P., and Weiss, A. 1986, *Astron. Astrophys.*, **164**, 237.
- Udalski, A. 2003, *Acta Astron.*, **53**, 291.
- Udalski, A., *et al.* 2005, *Astrophys. J. Letters*, **628**, L109.
- Udalski, A., Szymański, M., Kaluzny, J., Kubiak, M., Mateo, M., Krzemiński, W., and Paczyński, B. 1994, *Acta Astron.*, **44**, 227.
- Wyrzykowski, Ł. 2005, *PhD Thesis*, , Warsaw University Astronomical Observatory.

Appendix

Binary Lens Models

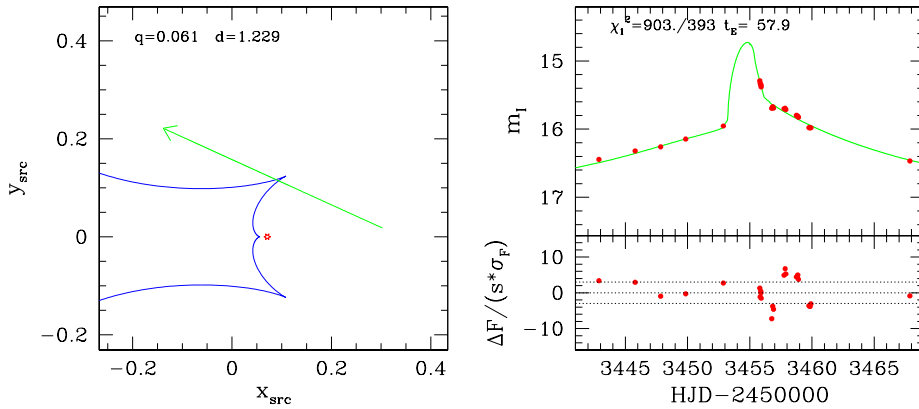
Below we present the plots for the 12 events for which the binary lens modeling has been applied. Some of the events, especially cases without apparent caustic crossing, may have alternative double source models. In such cases we show the comparison of the binary lens and double source fits to the data in the next subsection.

The events are ordered and named according to their position in the OGLE EWS database for the season 2005. We include two models for OGLE 2005-BLG-017 event, despite the huge difference in their formal fit quality, to show that it is possible to model the highly amplified part of the light curve with a binary lens. Alternative models of the event OGLE 2005-BLG-327 have different caustic topology.

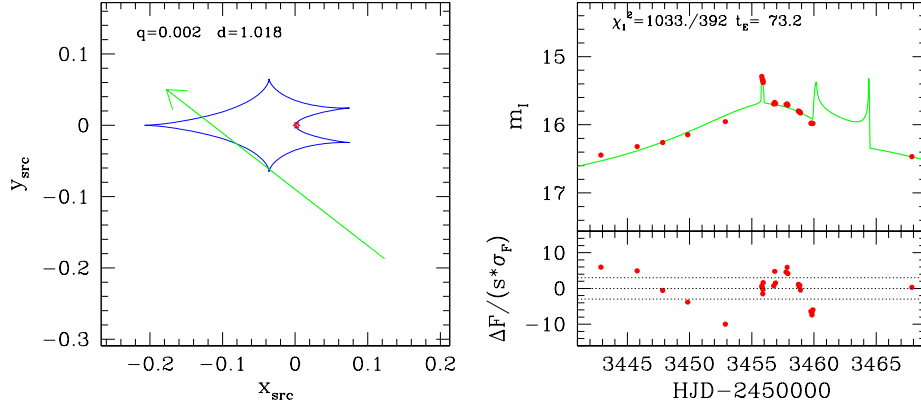
Each case is illustrated with two panels. The most interesting part of the source trajectory, the binary and its caustic structure are shown in the left panel for the case considered. The labels give the q and d values. On the right the part of the best fit light curve is compared with observations. The labels give the rescaled χ_1^2/DOF values. The source radius (as projected into the lens plane and expressed in Einstein radius units) is labeled only for the events with resolved caustic crossings. Below the light curves we show the differences between the observed and modeled flux in units of rescaled errors. The dotted lines show the rescaled $\pm 3\sigma$ band.

In all cases we plot the source trajectories in the coordinate systems of the binary lenses. In the case of OGLE 2005-BLG-018 the caustic structure shown corresponds to the binary separation when source passes the binary center of mass. The effects of rotation on the source path are so weak, that it is impossible to notice them in the plot.

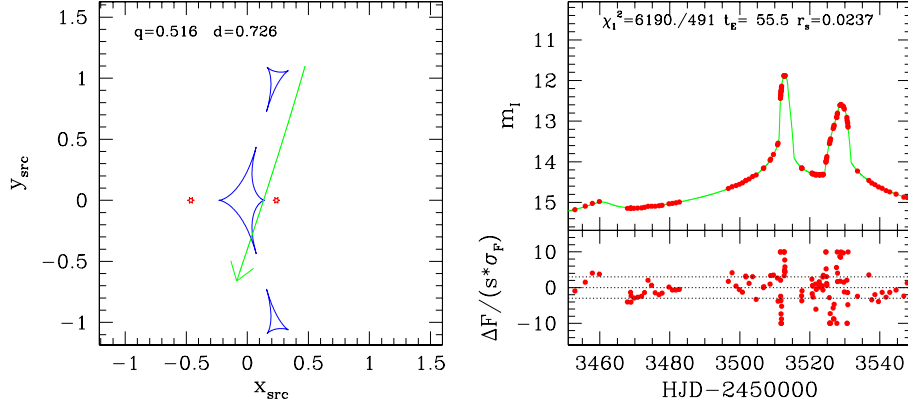
OGLE 2005-BLG-017 (best fit)



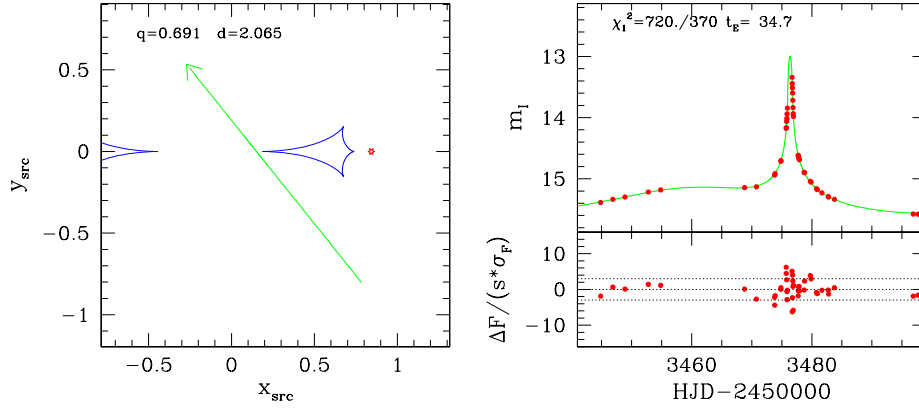
OGLE 2005-BLG-017 (another model)



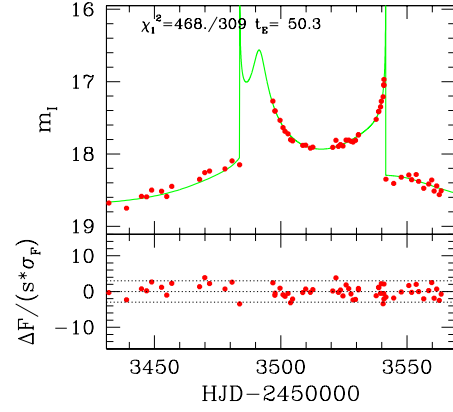
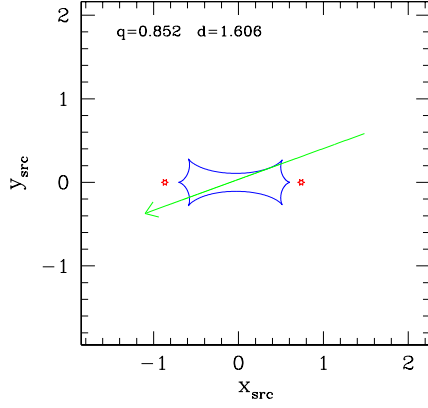
OGLE 2005-BLG-018



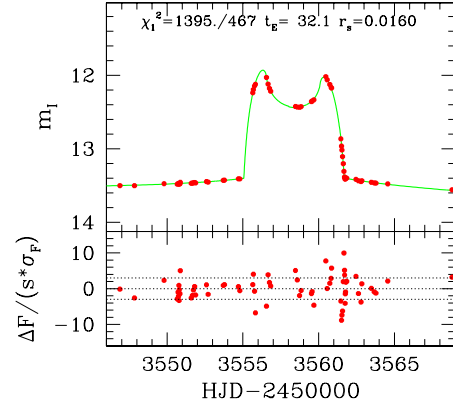
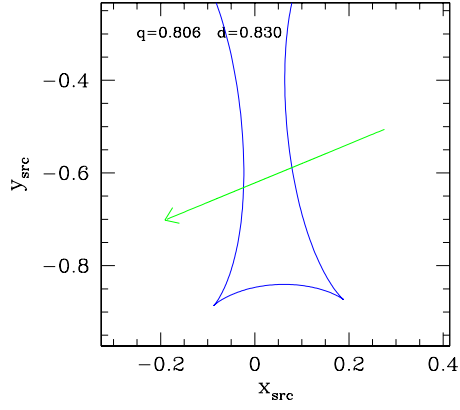
OGLE 2005-BLG-062



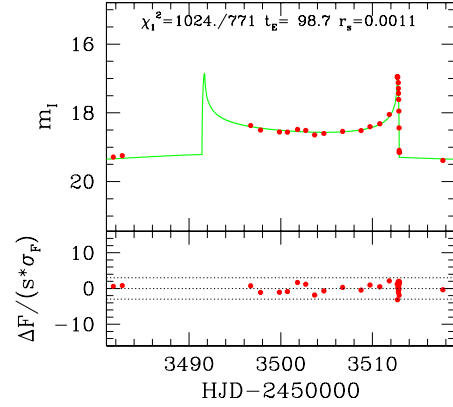
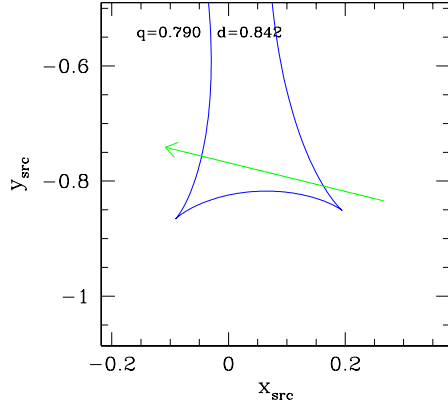
OGLE 2005-BLG-128

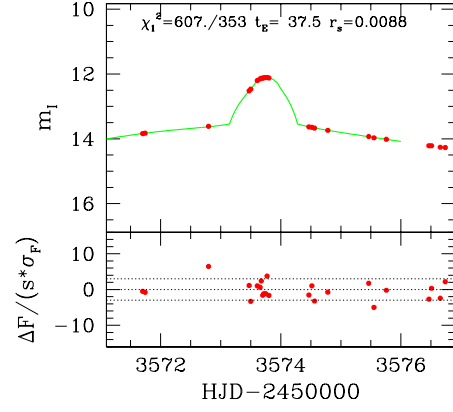
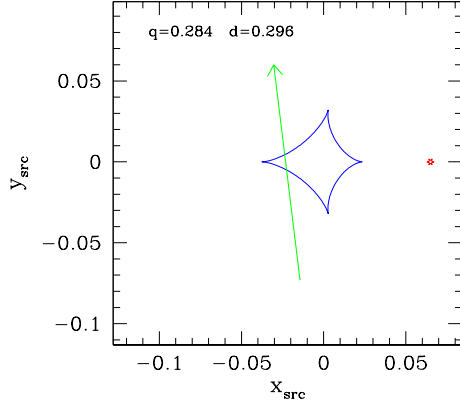
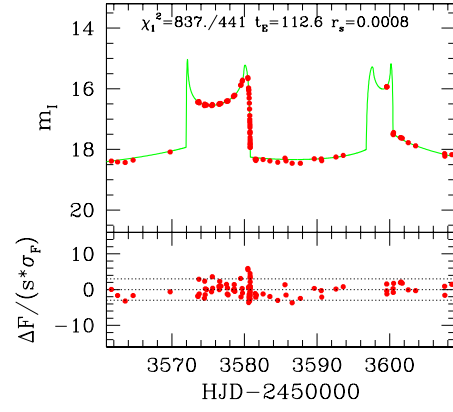
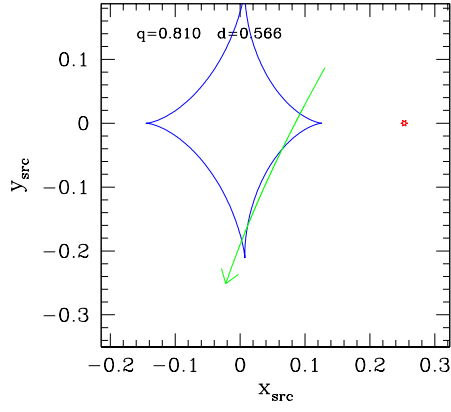
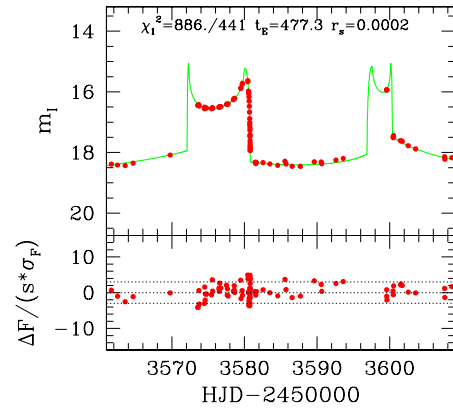
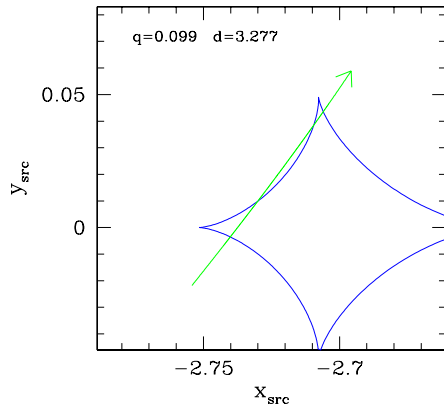


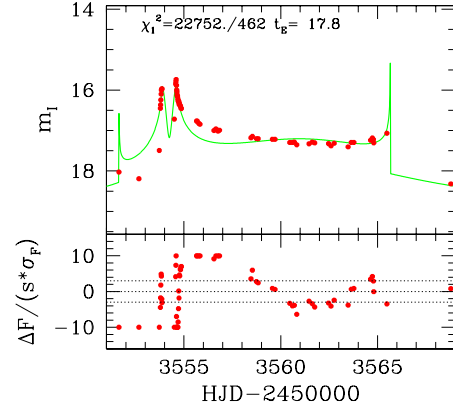
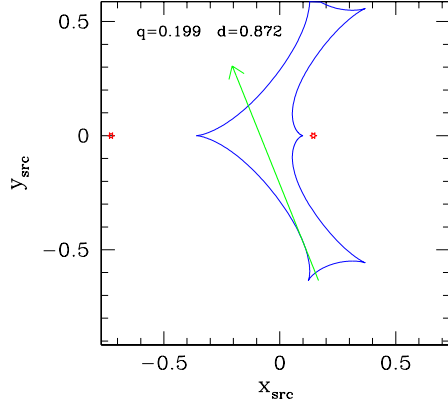
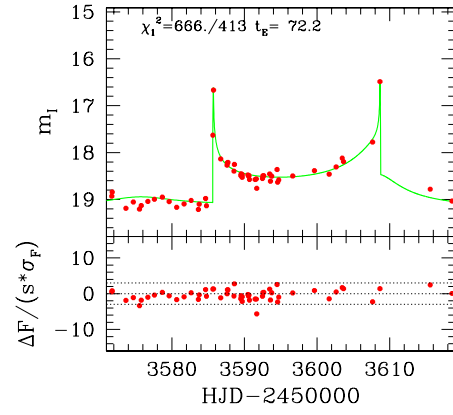
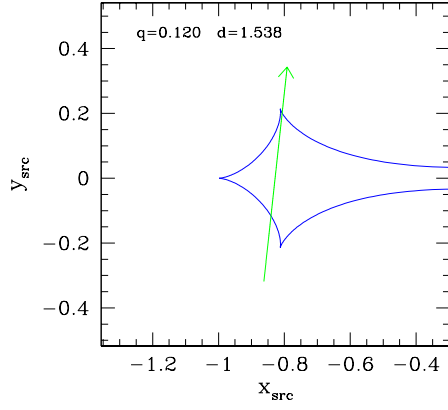
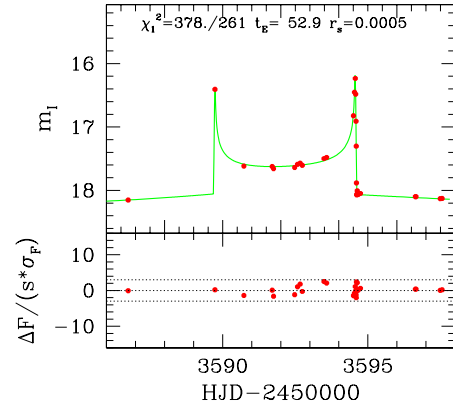
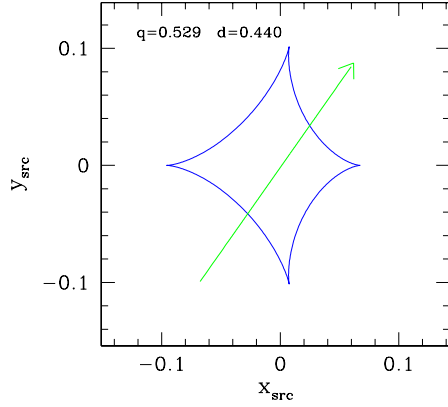
OGLE 2005-BLG-153

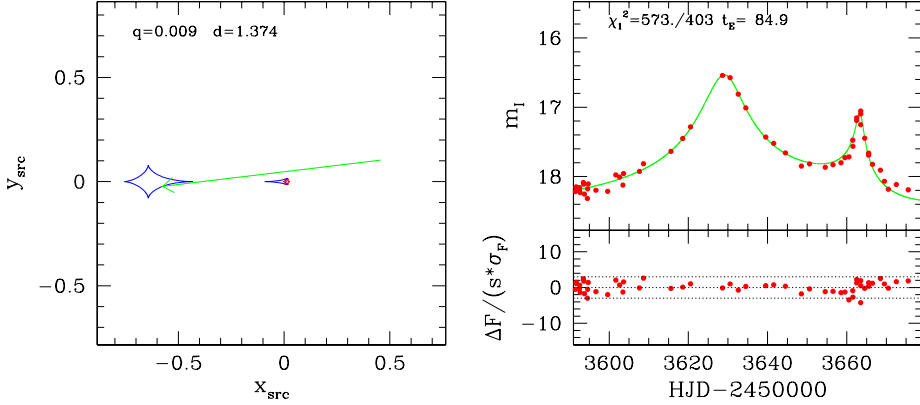


OGLE 2005-BLG-189

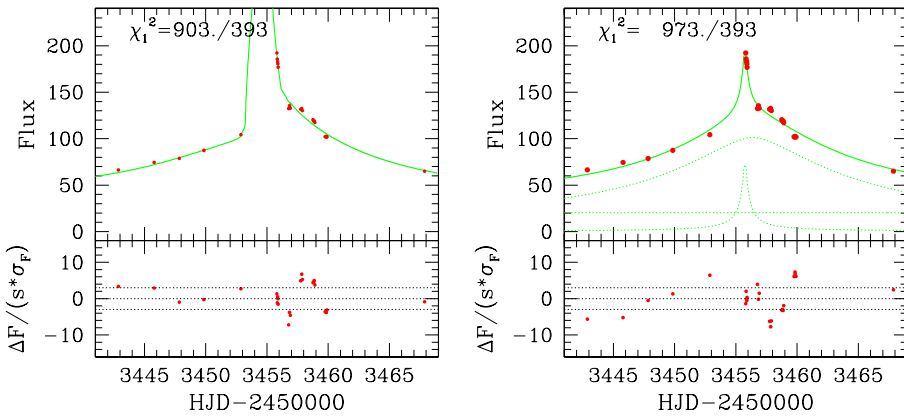


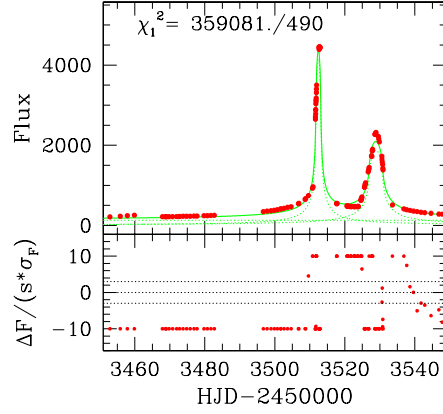
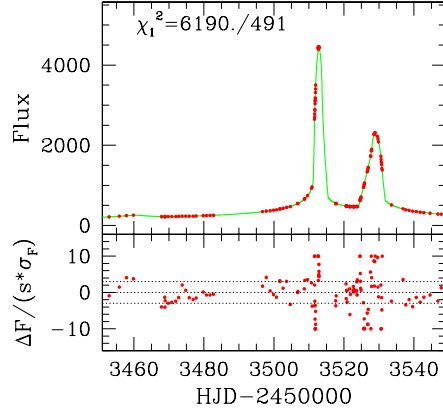
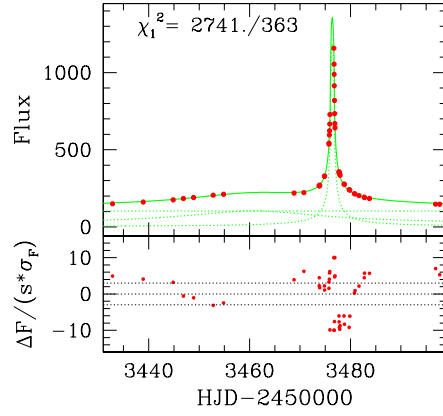
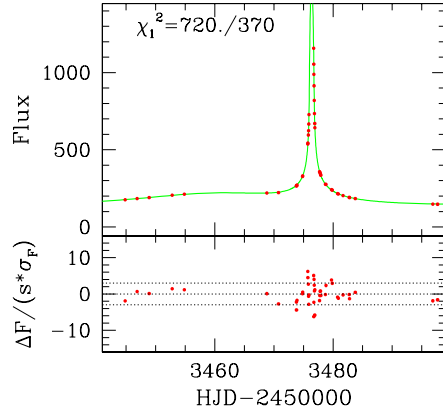
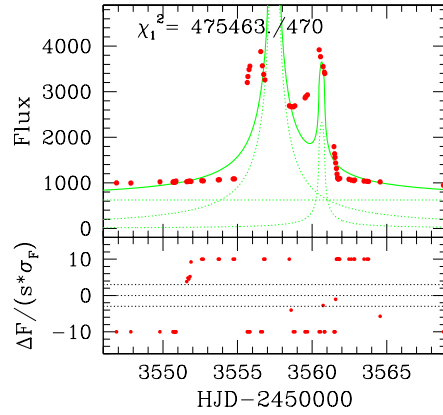
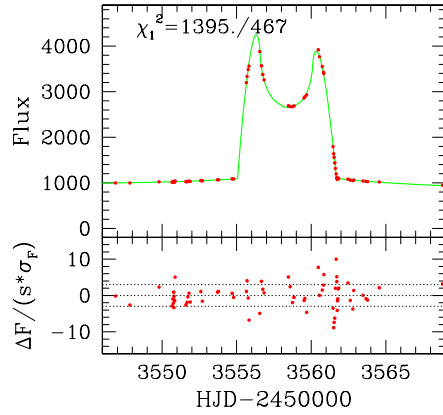
OGLE 2005-BLG-226**OGLE 2005-BLG-327 (close)****OGLE 2005-BLG-327 (wide)**

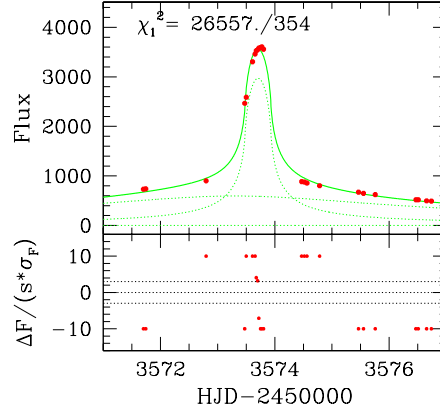
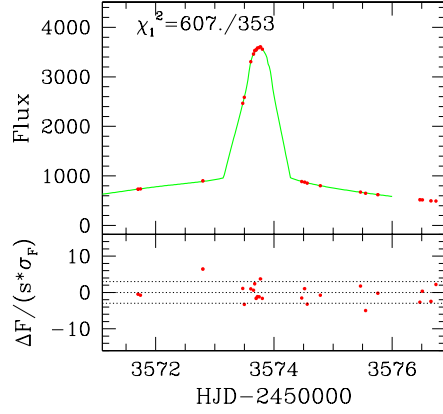
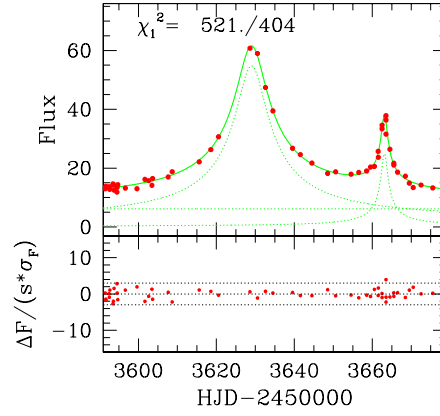
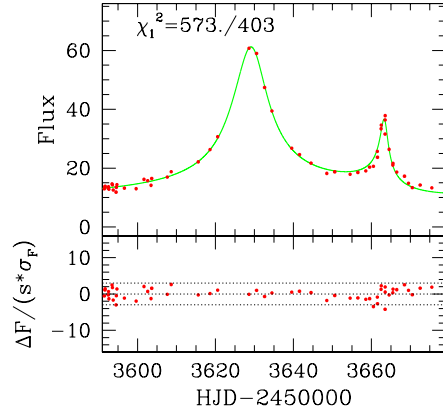
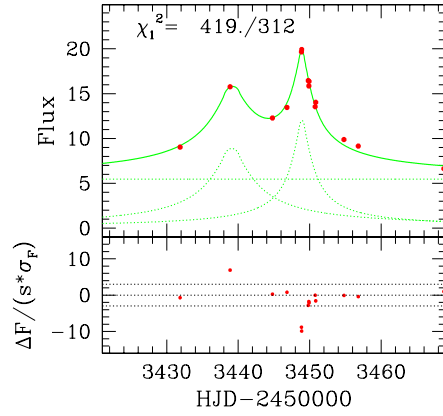
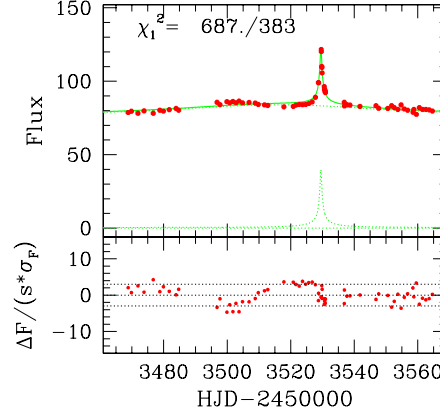
OGLE 2005-BLG-331**OGLE 2005-BLG-463****OGLE 2005-BLG-468**

OGLE 2005-BLG-477*Comparison of Binary Lens and Double Source Models*

Below we show the binary lens (on the left) and double source (on the right) models of the light curves for some of the considered events. For all binary lens models we have also calculated double source models. We do not show events with evident jumps in the light curves, which can only be modeled as caustic crossings. We include, however, a few cases with almost smooth observed light curves, despite the fact that their binary lens models are formally far better. The light curve in a double source model is a sum of the constant blended flux plus the two single lens light curves for the source components, each shown with dotted lines. In the plots we use observed fluxes (not magnitudes) since they are additive, which is important in double source modeling. In the majority of cases the binary lens models give formally better fits as compared to the double source models presented. On the other hand double source models, always producing simpler light curves, look more natural in some cases.

OGLE 2005-BLG-017

OGLE 2005-BLG-018**OGLE 2005-BLG-062****OGLE 2005-BLG-153**

OGLE 2005-BLG-226**OGLE 2005-BLG-477***Double Source Events***OGLE 2005-BLG-066****OGLE 2005-BLG-192**

Unsuccessful Fit
OGLE 2005-BLG-331

